Applied Catalysis B: Environmental 328 (2023) 122536

Contents lists available at ScienceDirect

Applied Catalysis B: Environmental

journal homepage: www.elsevier.com/locate/apcatb

Sodium ion intercalation in vanadium oxide promotes low-temperature NH_3-SCR activity: Sodium vanadium bronzes ($Na_{0.33}V_2O_5$) for NOx removal

Yusuke Inomata [a], Hiroe Kubota [b], Yoshinori Honmatsu [c], Hiroaki Takamitsu [c], Sosuke Sakotani [c], Kazuhiro Yoshida [c], Takashi Toyao [b], Ken-ichi Shimizu [b], Toru Murayama [d,e,*]

[a] Faculty of Advanced Science and Technology, Kumamoto University, Kumamoto 860-8555, Japan
[b] Institute for Catalysis, Hokkaido University, Sapporo, Hokkaido 001-0021, Japan
[c] Energia Economic and Technical Research Institute, the Chugoku Electric Power Company, Incorporated, Higashi-Hiroshima, Hiroshima 739-0046, Japan
[d] Research Center for Hydrogen Energy-based Society, Graduate School of Urban Environmental Sciences, Tokyo Metropolitan University, Hachioji, Tokyo 192-0397, Japan
[e] Yantai Key Laboratory of Gold Catalysis and Engineering, Shandong Applied Research Center of Gold Nanotechnology (Au-SDARC), School of Chemistry & Chemical Engineering, Yantai University, Yantai 264005, China

ARTICLE INFO

Keywords:
NH_3-SCR
NOx removal
Vanadium oxide
Vanadium bronzes

ABSTRACT

NH_3-SCR (selective catalytic reduction) is a key technique for converting harmful NOx to harmless N_2 and H_2O in exhaust gases. Herein, V_2O_5, $Na_{0.33}V_2O_5$ and $Na_{1.2}V_3O_8$ are synthesized by a simple chemical process (the oxalate method) as examples of Na-intercalated vanadium oxide (sodium vanadium oxide bronze) for low-temperature NH_3-SCR less than 150 °C. Among them, $Na_{0.33}V_2O_5$ shows 92% (dry) and 86% (in the presence of 10 vol% water) NO conversions at 150 °C. The reaction rate of $Na_{0.33}V_2O_5$ is 6.1-times higher than that of V_2O_5, indicating that Na intercalation accelerates NH_3-SCR cycles. Mechanistic analysis suggests that the reaction mechanism of $Na_{0.33}V_2O_5$ is different from those of other V-based catalysts. Although it has been believed that alkali ions inhibit catalytic cycles of NH_3-SCR, the results of this study suggest that alkali ions affect the structural, redox and adsorption properties of bulk V_2O_5, leading to an increase in NH_3-SCR activity.

1. Introduction

NOx (NO and NO_2) removal is an important process for the chemical industry because NOx is a harmful gas that causes acid rain and photochemical smog as well as respiratory disease, and its release into the atmosphere must be suppressed. NH_3-SCR (selective catalytic reduction) has been used for NOx removal from stationary sources (such as waste treatment plants and coal-fired power plants). In this reaction, ammonia works as a reducing reagent to convert harmful NOx to harmless N_2 and H_2O [1,2].

$$4NO + 4NH_3 + O_2 \rightarrow 4\ N_2 + 6\ H_2O \quad (1)$$

Although various redox active metal oxides such as V [2], Mn [3,4], Cr [4], Cu [4], Mo [5,6], W [7], Ce [7], Sn [8] and Fe-oxides [9] have been investigated for low-temperature NH_3-SCR activity, vanadia-based catalysts have good chemical stability, N_2 selectivity and tolerance to SO_2 that exists in exhaust gas and they have therefore been used for commercial catalysts (V_2O_5/TiO_2, V_2O_5-WO_3/TiO_2, etc.) [2]. However, current vanadia-based catalysts require a temperature of more than 300 °C for NH_3-SCR to proceed [10,11]. For this reason, SCR catalysts are always placed upstream of exhaust gas treatment systems where the temperature of the gas is high (>300 °C) and they are exposed to untreated exhaust gas containing ash and SO_2. As a result, the catalysts are deactivated because of blockage of active sites by physical deposition of ash or sulfate ($(NH_4)_2SO_4$, $(NH_4)HSO_4$) caused by vanadia-catalyzed SO_2 oxidation followed by reaction with NH_3. Therefore, these drawbacks must be overcome and catalysts that show low temperature (>150 °C) NH_3-SCR activity are required.

Recently, the importance of crystalline vanadium oxide for low-temperature NH_3-SCR has been reported. Lian et al. reported that the crystalline V_2O_5/TiO_2 catalyst calcined at high temperature (850 °C) proceeds with low-temperature NH_3-SCR (~180 °C) by the unique mechanism accompanied by the structural changes of vanadium species. [12] In contrast to supported vanadium catalysts, we previously

* Corresponding author at: Research Center for Hydrogen Energy-based Society, Graduate School of Urban Environmental Sciences, Tokyo Metropolitan University, Hachioji, Tokyo 192-0397, Japan.
E-mail address: murayama@tmu.ac.jp (T. Murayama).

https://doi.org/10.1016/j.apcatb.2023.122536
Received 30 October 2022; Received in revised form 22 January 2023; Accepted 23 February 2023
Available online 24 February 2023

reported that bulk V_2O_5-based catalysts exhibit greater NH_3-SCR activity than that of conventional TiO_2-supported V_2O_5 catalysts because of their faster redox cycles [13–17]. Furthermore, mixed-valence VOx (V^{4+} + V^{5+}) catalysts were synthesized by changing their calcination conditions and they showed > 99% NO conversion at 150 °C (250 ppm NO, 250 ppm NH_3, 4% O_2, SV=40,000 mL h^{-1} g_{cat}^{-1}) by the Lewis acid mechanism [14]. Therefore, the coexistence of V^{4+} and V^{5+} would contribute to the enhancement of low-temperature NH_3-SCR activity.

The structural flexibility of vanadium oxide is greater than that of other oxides because of various charge states (V^{5+}, V^{4+}, V^{3+} and V^{2+}), redox couples (ex. V^{4+}/V^{5+}), and various vanadium coordination environments (octahedra, distorted octahedra, square pyramids and tetrahedra), leading to a variety of crystal phases including mixed valence oxides and complex oxides [18]. Among the V-based complex oxides, vanadium oxide bronzes ($A_xV_xO_y$) are non-stoichiometric compounds that are composed of vanadia moieties and other cations (Li^+ [18], Na^+ [19], Mg^{2+} [20], Zn^{2+} [21], Cu^{2+} [22], NH^{4+} [23], etc.). Vanadium oxide bronzes adopt tunnel (β-$A_xV_2O_5$) or layered type (α-$A_xV_2O_5$, δ-$A_xV_2O_5$, γ-$A_xV_2O_5$) crystal structures and they host metal cations in the tunnel structure or between the layers [18]. As a result, vanadium oxide bronzes have a mixed valence state (V^{4+} and V^{5+}) owing to accessible V^{4+}/V^{5+} redox couples. Furthermore, vanadium oxide bronzes show metallic properties, while V_2O_5 exhibits semiconducting properties. Among the vanadium oxide bronzes, sodium vanadium bronzes (Na-intercalated vanadium oxides) are well-known V-based bronze materials, and $Na_{0.33}V_2O_5$ and $Na_{1.2}V_3O_8$ are known as their stable phases [19,24,25]. It has been believed that alkali ions are blocked acid sites of vanadium oxide to inhibit the adsorption of NH_3 and deactivate NH_3-SCR activity [26–29]. However, in terms of controlling structural and electronic properties, intercalation of Na ions in vanadium oxide modulates the crystal structure and the charge state of vanadium cations (ratio of V^{4+}/V^{5+}), and that would be a promoter of NH_3-SCR activity.

Here, we report sodium vanadium bronzes as low-temperature NH_3-SCR catalysts that show high activity at a temperature below 150 °C. Na-intercalated vanadium oxide catalysts are synthesized by simple chemical routes (the oxalate method) that are easier than previously reported methods such as hydrothermal methods and solid-state synthesis [30–32]. NH_3-SCR activities of the catalysts with different amounts of Na were measured under dry and wet (10 vol% water) conditions and their reaction mechanism was investigated.

2. Experimental section

2.1. Reagents

Ammonium metavanadate (NH_4VO_3), oxalic acid and sodium nitrate ($NaNO_3$) were purchased from FUJIFILM Wako Pure Chemical Corporation. All reagents were used without further purification.

2.2. Synthesis of Na-intercalated vanadium oxide catalysts

First, NH_4VO_3 and oxalic acid (11.9 g, 131.7 mmol) were dissolved in 50 mL of water and the aqueous solution was stirred for 10 min for completion of the change in color of the solution. Next, $NaNO_3$ was added to the solution. Then the solution was heated overnight to evaporate the water on a hotplate. Finally, the resulting solid was calcined twice at 300–600 °C for 4 h each time. Different Na-intercalated vanadium oxide catalysts (xmol% Na-intercalated vanadium oxides, xNa-V) were synthesized by changing the amounts of NH_4VO_3 and $NaNO_3$. The amounts of reagents are shown in Table S1. For comparison, 1 wt% V_2O_5–5 wt% WO_3/TiO_2 (V-W/TiO_2) was prepared as a model of the conventional catalyst (see supporting information for the preparation). W-substituted V_2O_5 (3.5 mol% W) was synthesized according to our previous report [17].

2.3. Catalyst characterization

X-ray diffraction (XRD) patterns were collected by SmartLab (Rigaku) with Cu Kα radiation. The crystal structure was drawn by VESTA [33]. The molar ratio of Na to V (Na: V) was measured by the inductively coupled plasma (ICP) atomic emission spectroscopy observation. The specific surface areas of the catalysts were calculated by N_2 adsorption measurements and the Brunauer-Emmett-Teller (BET) equation using MicrotracBEL, BELSORP-max. For N_2 adsorption measurements, 100 mg of the catalyst was put into a quartz sample tube. UV–vis spectra of catalysts were measured by using Shimadzu UV-3100PC equipped with an integrating sphere attachment (ϕ=150 mm), Shimadzu ISR-3100. For diffuse reflectance spectra measurements, samples were pressed on a board of barium sulfate.

2.4. Catalytic activity test

The NH_3-SCR activity of vanadium oxide catalysts was measured using a fixed-bed flow reactor (Scheme S1). The reaction gas mixture, 250 ppm NO, 250 ppm NH_3, 4 vol% O_2 and 10 vol% water (when used) in Ar (250 mL min^{-1}), was fed to the catalyst (0.375 g). The outlet gases were analyzed by an IR spectrometer (JASCO FT/IR-4700) equipped with a gas cell (JASCO LPC12M-S). NO conversion and N_2 selectivity were calculated by the following equations.

$$\text{NO conversion}(\%) = \frac{NO_{in} - NO_{out}}{NO_{in}} \times 100 \quad (2)$$

$$N_2\text{selectivity}(\%) = \frac{2 * N_{2out}}{(NO_{in} + NH_{3in}) - (NO_{out} + NH_{3out})} \quad (3)$$

$$(2 * N_{2out} = (NO_{in} + NH_{3in}) - (NO_{out} + NH_{3out} + NO_{2_{out}} + 2 * N_2O_{out}))$$

The reaction rate and reaction order of the catalysts were determined by adjusting the amount of catalysts and the flow rate for NO conversion to be below 20%.

2.5. Mass spectra measurements

Prior to measurements, the samples (each 40 mg) were heated under a flow of 10% O_2 / He (100 mL min^{-1}) at 300 °C for 10 min. Then the reaction gas mixture was introduced to the sample at a flow rate of 100 mL min^{-1}. The sequence of flowing gases is shown in the caption of Fig. 4 The outlet gas was analyzed by a mass spectrometer (BELMass, MicrotracBEL Corp.).

2.6. NH_3 and NO temperature-programmed desorption measurements

NH_3 and NO temperature-programmed desorption (NH_3-TPD and NO-TPD) measurements were conducted by using MicrotracBEL BELCAT II. For NH_3- and NO-TPD, 100 mg of the catalyst was put in a quartz sample tube. For NH_3-TPD measurement, pretreatment was conducted under a He flow (250°C, 1 h) and NH_3/He (5%) for adsorption (100°C, 1 h) followed by purging with He (100°C, 1 h). For NO-TPD measurement, NO/He (2000 ppm) was used for the adsorption gas. Then TPD profiles were recorded with increases in temperature (20°C /min) under He flow using a mass spectrometer ($m/z = 17$ for NH_3-TPD and $m/z = 30$ for NO-TPD).

2.7. Temperature-programmed surface reaction measurements

Temperature-programmed surface reaction (TPSR) profiles were obtained by using MicrotracBEL BELCAT. A mass spectrometer (BELMass, MicrotracBEL Corp.) was used for the analysis of outlet gases. Samples (each 40 mg) were placed in a quartz tube. The samples were heated (20°C / min) under a gas mixture (500 ppm NH_3 + 500 ppm NO / He) flow.

3. Results and discussion

3.1. Characterization of vanadium bronze catalysts synthesized by the oxalate method

3.1.1. XRD patterns and structures of vanadium bronze catalysts

Na-intercalated vanadium oxide catalysts (xNa-V) were synthesized by the oxalate method using ammonium metavanadate (NH_4VO_3), oxalic acid and sodium nitrate ($NaNO_3$) as precursors. In this process, vanadium-oxalate complexes were formed and Na was then intercalated by the calcination steps.

First, powder XRD observations were conducted to check the crystal structures of vanadium oxide catalysts with different amounts of sodium calcined at 300 °C (Fig. 1). For the 0Na-V sample (without Na), the XRD patterns showed orthorhombic V_2O_5 (α-V_2O_5) without impurity diffraction peaks (Fig. 1***b, structure (1)***). For 8Na-V, mixed patterns of V_2O_5 and $Na_{0.33}V_2O_5$ (Fig. 1***b, structure (2)***) were confirmed. When the molar ratio of Na was increased up to 16 mol%, the XRD patterns of the catalyst (16Na-V) were assigned to single-phase $Na_{0.33}V_2O_5$. From ICP atomic emission spectroscopy measurements for 16Na-V, the molar ratio of Na to V (Na: V) was 0.32: 2.0, which was close to the theoretical value (Na: V = 0.33: 2.0). Mixed patterns of $Na_{0.33}V_2O_5$ and $Na_{1.2}V_3O_8$ (Fig. 1***b, structure (3)***) were observed for 23Na-V and 33Na-V. Single XRD patterns of $Na_{1.2}V_3O_8$ were confirmed when 50 mol% of Na was introduced into V_2O_5 (50Na-V). Thus, the crystal phases of these catalysts changed depending on the amount of Na. Sodium vanadium bronzes obtained by our preparation method are easily formed at a lower temperature (300 °C) compared to previously reported methods such as hydrothermal methods and solid phase methods [30–32]. For 16Na-V ($Na_{0.33}V_2O_5$), the XRD patterns were the same regardless of their calcination temperatures (300–600 °C, Fig. S1).

As shown in Fig. 1***b***, the configurations and coordination numbers of vanadium units changed with change in the molar ratio of Na [18]. α-V_2O_5 is composed of corner and edge-sharing square pyramidal VO_5 units. Vanadium moieties of $Na_{0.33}V_2O_5$ consist of chains of edge-sharing VO_5 square pyramids and chains of edge-sharing VO_6 octahedra. These chain moieties are connected by corner-sharing and they form tunnel structures in which Na ions are intercalated. $Na_{1.2}V_3O_8$ is also composed of chains of edge-sharing VO_5 square pyramids and chains of edge-sharing VO_6 octahedra but has a layered structure, and Na ions exist between the layers. These structural differences would affect the catalytic activity.

3.1.2. Specific surface area of vanadium bronze catalysts

Specific surface areas of xNa-V catalysts were checked from N_2 adsorption measurements. For single-phase catalysts, the specific surface area of V_2O_5 (0Na-V) was 41 m^2/g, while the specific surface area of 16Na-V ($Na_{0.33}V_2O_5$) was 26 m^2/g. The value decreased to 18 m^2/g for 50Na-V ($Na_{1.2}V_3O_8$). Therefore, the specific surface area of the catalysts decreased with an increase in the amount of Na introduced. The specific surface areas of other catalysts are shown in supporting information (Fig. S2). The specific surface areas of $Na_{0.33}V_2O_5$ calcined at different temperatures are also shown in Fig. S3. The specific surface area of $Na_{0.33}V_2O_5$ calcined at 300 °C was 26 m^2/g and the specific surface area decreased with an increase in calcination temperature.

3.2. NH_3-SCR activity of vanadium bronze catalysts

3.2.1. Relationship between NH_3-SCR activity and amount of sodium

The catalytic activities of Na-intercalated V_2O_5 (xNa-V) were measured under dry and wet (10 vol% water) conditions at 150 °C. Fig. 2***a*** shows the relationship between the amount of Na and NO conversions. V_2O_5 (0Na-V, 0Na-V) showed NO conversions of 82% (dry) and 47% (wet). When the amount of Na was increased, $Na_{0.33}V_2O_5$ (16Na-V) exhibited 92% (dry) and 86% (wet) NO conversions. The activity of $Na_{0.33}V_2O_5$ (16Na-V) increased and its NO conversion was less affected by water vapor, although the value of its specific surface area (26 m^2/g) decreased compared to that of V_2O_5 (41 m^2/g). On the other hand, the NO conversions of $Na_{1.2}V_3O_8$ (50Na-V) were 70% (dry) and 42% (wet) and thus the NH_3-SCR activity of $Na_{1.2}V_3O_8$ was lower than those of V_2O_5 (0Na-V) and $Na_{0.33}V_2O_5$ (16Na-V). $Na_{0.33}V_2O_5$ and $Na_{1.2}V_3O_8$ are mixed-valence metal oxides and the ideal charge states of vanadium are + 5.000 (V_2O_5), + 4.835 ($Na_{0.33}V_2O_5$) and + 4.933 ($Na_{1.2}V_3O_8$). According to our previous report, V^{4+} sites enhance the NH_3-SCR activity and mixed-valence vanadium oxides showed greater activity than that of V_2O_5 [14]. Therefore, V^{4+}-rich $Na_{0.33}V_2O_5$ would show the best NH_3-SCR activity.

3.2.2. Effect of calcination temperature on NH_3-SCR activity of $Na_{0.33}V_2O_5$

The effect of calcination temperature for $Na_{0.33}V_2O_5$ (16Na-V) was investigated (Fig. 2***b***). When the calcination temperatures were 300–400 °C, the NO conversions of the catalysts were the same. The NO conversions of $Na_{0.33}V_2O_5$ decreased to < 60% (dry) and < 50% (wet) when it was calcined at 450 °C and 500 °C. $Na_{0.33}V_2O_5$ calcined at 600 °C showed only 7% (dry) and 12% (wet) NO conversions. This change in activity can be attributed to both the electronic state of V on the surfaces and the specific surface area.

3.2.3. Relationship between catalytic activity ($Na_{0.33}V_2O_5$, V_2O_5 and conventional catalyst) and reaction temperature

We also investigated the dependence of NO conversions on reaction temperature for $Na_{0.33}V_2O_5$ (16Na-V), V_2O_5 (0Na-V) and a model of

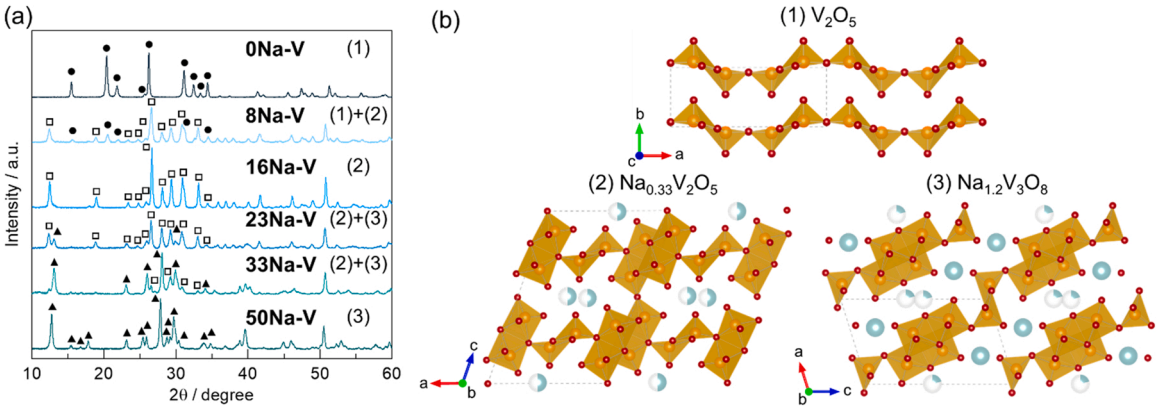

Fig. 1. (a) XRD patterns of sodium ion-intercalated vanadium oxide catalysts. Symbols: V_2O_5 (•), $Na_{0.33}V_2O_5$ (□) and $Na_{1.2}V_3O_8$ (▲). (b) Crystal structures of V_2O_5 (1), $Na_{0.33}V_2O_5$ (2) and $Na_{1.2}V_3O_8$ (3). Orange sphere: V atoms, red sphere: O atoms, light blue: Na atoms. Occupancy of Na atoms is shown by the ratio of the light blue part to the white part.

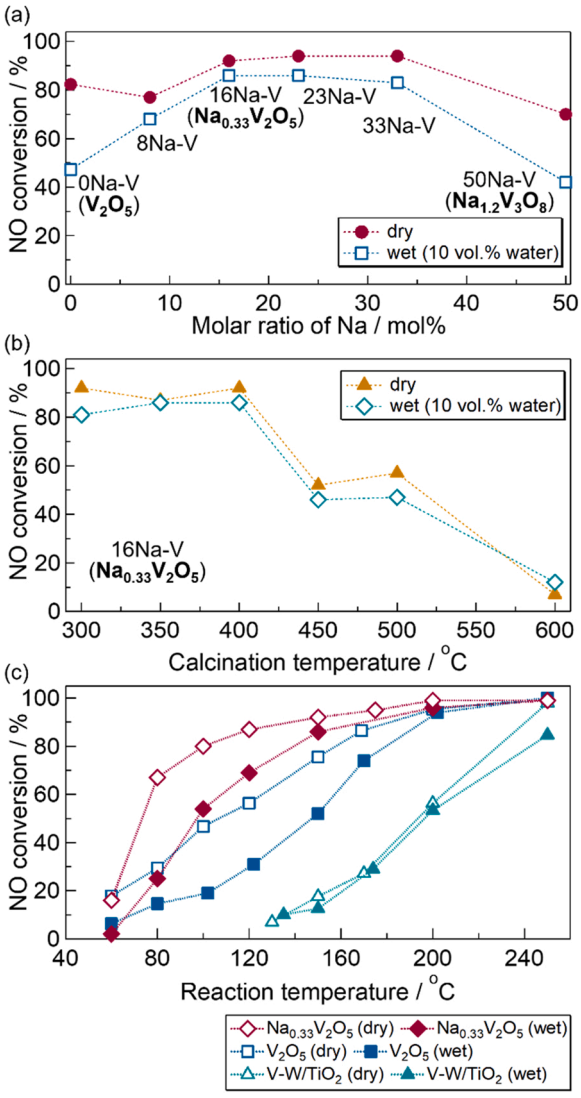

Fig. 2. (a) NO conversion (150 °C) of sodium ion-intercalated vanadium oxide catalysts as a function of the molar ratio of sodium. (b) NO conversion (150 °C) of $Na_{0.33}V_2O_5$ (16Na-V) as a function of the calcination temperature. (c) NO conversion of $Na_{0.33}V_2O_5$ (16Na-V), V_2O_5 (0Na-V, without sodium ions) and V-W/TiO_2 (model of a conventional catalyst) as a function of reaction temperature. Reaction conditions: amount of catalyst, 0.375 g; reaction gas mixture, 250 ppm NO, 250 ppm NH_3, 4 vol% O_2 and 10 vol% H_2O (when used) in Ar; flow rate, 250 mL min^{-1}; space velocity, 40,000 mL h^{-1} g_{cat}^{-1}.

conventional catalysts (TiO_2-supported V_2O_5-WO_3 catalyst, V-W/TiO_2). The temperatures for 80% NO conversion (T_{80}) were 100 °C ($Na_{0.33}V_2O_5$), 157 °C (V_2O_5), and 225 °C (V–W/TiO_2) under a dry condition and 138 °C ($Na_{0.33}V_2O_5$), 178 °C (V_2O_5), and 236 °C (V–W/TiO_2) under a wet (10 vol% water) condition (Fig. 2***c***). Notably, $Na_{0.33}V_2O_5$ showed 67% NO conversion at 80 °C under a dry condition. N_2 selectivity of $Na_{0.33}V_2O_5$ was > 99% and no N_2O formation was confirmed (Fig. S4). Thus, $Na_{0.33}V_2O_5$ showed greater low-temperature NH_3-SCR activity than that of V_2O_5 (without Na) and a conventional catalyst.

3.2.4. Reaction rates of $Na_{0.33}V_2O_5$ for NH_3-SCR

Reaction rates (per specific surface area) of the catalysts were measured to compare the activities of surface reaction sites under kinetic control. Fig. 3 shows the reaction rate of $Na_{0.33}V_2O_5$, W-substituted V_2O_5 (W-V_2O_5) that we previously reported [17], V_2O_5 (without any substituted or intercalated metals) and the conventional catalyst (V–W/TiO_2). Reaction rates per specific surface area were 1.96×10^{-8} ($Na_{0.33}V_2O_5$), 5.17×10^{-9} (W-V_2O_5), 3.22×10^{-9} (V_2O_5) and 2.19×10^{-10} mol_{NO} m^{-2} s^{-1} (V–W/TiO_2) in a dry condition. The reaction rate of $Na_{0.33}V_2O_5$ was 89-times higher than that of the conventional V–W/TiO_2 catalyst. In the presence of water vapor (10 vol% H_2O), the values were 2.03×10^{-8} ($Na_{0.33}V_2O_5$), 4.19×10^{-9} (W-V_2O_5), 1.37×10^{-9} (V_2O_5) and 1.93×10^{-10} mol_{NO} m^{-2} s^{-1} (V–W/TiO_2). These results indicate that the reaction cycles of $Na_{0.33}V_2O_5$ are less affected by water vapor. To compare the reactivity, the reaction, reaction rates per mol of surface vanadium atom was also calculated (Fig. S5). $Na_{0.33}V_2O_5$ showed the largest reaction rate as well as reaction rates per specific surface area.

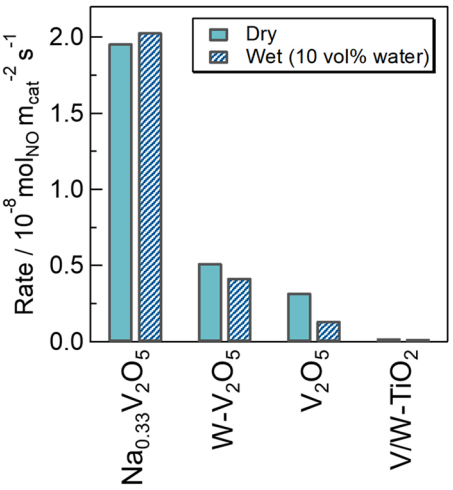

Fig. 3. Reaction rates per specific surface area at 150 °C for $Na_{0.33}V_2O_5$ (16Na-V), W-V_2O_5 (W-substituted vanadium oxide), V_2O_5 (without any additional ions) and V-W/TiO_2 (model of a conventional catalyst) at 150 °C.

3.3. Reaction mechanism of vanadium bronzes for NH_3-SCR

3.3.1. Reaction orders and apparent activation energies of $Na_{0.33}V_2O_5$ for NH_3-SCR

The reaction mechanism of $Na_{0.33}V_2O_5$ was studied by kinetic measurement, TPD, TPR, MS observations and UV–vis spectra measurements. Reaction orders (150 °C) of $Na_{0.33}V_2O_5$ were 0.6 (NH_3), 1.0 (NO) and 0.4 (O_2) (Table 1 and Fig. S6***(a-c)***). The results indicate that reaction steps related to NO are rate-determining steps. Reaction orders for NO and O_2 were close to those previously reported for bulk V_2O_5-based catalysts (Table 1, W-V_2O_5 and V_2O_5).[17] For the reaction orders of NH_3 of vanadia-based catalysts, the values are generally close to 0 because of the strong acid-base interaction between NH_3 and acid sites on vanadia [2]. However, the reaction order of $Na_{0.33}V_2O_5$ for NH_3 was comparably large, indicating that the interaction between NH_3 and the surface is weakened or that the reaction step related to NH_3 might affect the reaction rates in which a rate-determining step is the reduction step of vanadium sites by NO + NH_3. The apparent activation energy of $Na_{0.33}V_2O_5$ was E_a = 20 kJ/mol from the Arrhenius plot (Fig. S6***(d)***) and that value was smaller than the values of V_2O_5 (E_a = 39 kJ/mol) and V/W-TiO_2 (E_a = 43 kJ/mol) [17], suggesting that $Na_{0.33}V_2O_5$ is

Table 1
Kinetic parameters of bulk vanadium oxide-based catalysts for NH_3-SCR.

Catalysts	Reaction orders			Apparent activation energy E_a / kJ mol^{-1}	Ref.
	NH_3	NO	O_2		
$Na_{0.33}V_2O_5$	0.6	1.0	0.4	20	This work
W-V_2O_5[a]	0.3	0.9	0.3	36	16
V_2O_5	0.3	1.0	0.3	39	16

[a] 3.5 mol%W-V_2O_5.

energetically favorable for the NH_3-SCR to proceed.

3.3.2. Mass spectra measurements

MS spectra were recorded under various gas flows in transient and steady states. Under an NO + NH_3 flow, the peak of N_2 production was initially confirmed, but it gradually decreased with an increase in MS intensities of NO and NH_3 (Fig. 4***a***). For N_2 production, the same behavior was observed under the condition of NH_3 adsorption followed by NO + O_2 flow (Fig. 4***b***). Under NO + NH_3 + O_2 flow (steady state), considerable N_2 production was confirmed, but the MS intensity of N_2 decreased when NH_3 was turned off (NO + O_2, Fig. 4***c***). These results indicate that NH_3, NO and O_2 participate in the catalytic production of N_2.

3.3.3. NH_3- and NO- TPD measurements of $Na_{0.33}V_2O_5$

NH_3- and NO-TPD observations were conducted to determine the adsorption properties of $Na_{0.33}V_2O_5$ to NH_3 and NO and its redox properties. For NH_3-TPD, the desorption peak of NH_3 was confirmed at a temperature of around 250 °C (Fig. 5***a***). The amount of NH_3 adsorbed per specific surface area was 1.9 μmol m^{-2} ($Na_{0.33}V_2O_5$). We previously reported that the value for V_2O_5 (without Na) synthesized by the same method (oxalate method) was 2.1 μmol m^{-2} [13]. Therefore, $Na_{0.33}V_2O_5$ has sufficient acid sites and Na intercalation does not block the acid sites. $Na_{0.33}V_2O_5$ showed a desorption peak of NO (350–550 °C) from NO-TPD measurement (Fig. 5***b***), although previous studies showed that NO does not adsorb on the surface of the catalysts during the SCR cycle for vanadia-based catalysts. Given that pure V_2O_5 (without Na) adsorbs NH_3 and O_2, NO might adsorb on Na sites and NO also adsorbs on the catalysts in addition to NH_3 and O_2, which is different from other vanadia-based catalysts.

3.3.4. Redoxability of $Na_{0.33}V_2O$ during NH_3-SCR

Redox of $Na_{0.33}V_2O_5$ during NH_3-SCR cycles was checked from UV–vis spectra observation before and after the NH_3-SCR activity test (Fig. 6). After NH_3-SCR, the adsorption around λ = 700 nm (d-d transition of V^{4+}) increased and the adoption edge was shifted to a lower wavelength (λ = 585 nm → 570 nm) [34,35]. These changes suggest reduction of vanadium sites. From the results of NH_3- and NO-TPD and UV–vis spectra measurement, $Na_{0.33}V_2O_5$ proceeds with the NH_3-SCR by the adsorption of NH_3 and NO, and the catalysts are partially reduced during the NH_3-SCR cycles.

The reduction abilities of $Na_{0.33}V_2O_5$ were evaluated from temperature-programmed surface reaction (TPSR) measurements under NH_3 + NO. N_2 production started at room temperature and production of N_2 and H_2O was observed up to 250 °C (Fig. 7***a***). Further N_2 and H_2O production was confirmed (>250 °C) and N_2O was produced as a by-

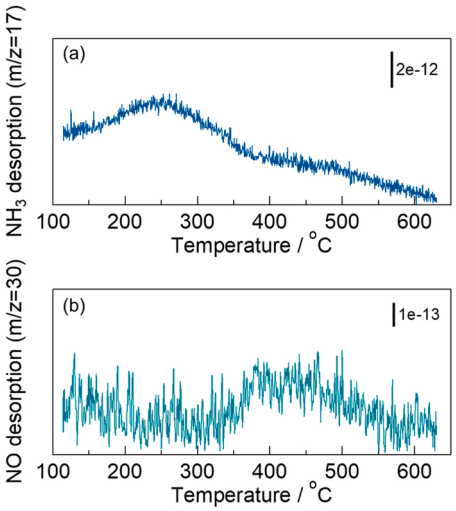

Fig. 5. (a) NH_3-TPD and (b) NO-TPD profiles of $Na_{0.33}V_2O_5$ (16Na-V).

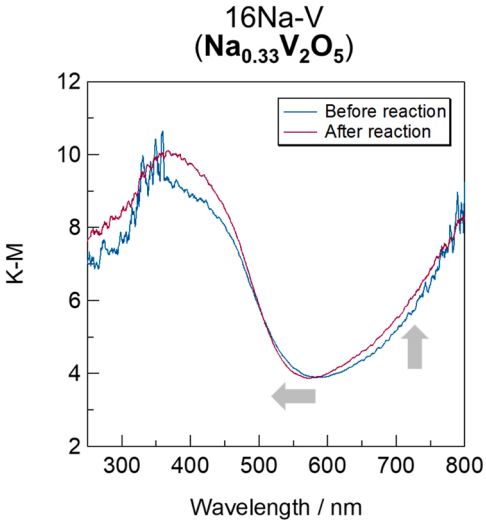

Fig. 6. UV–vis spectra of $Na_{0.33}V_2O_5$ before and after NH_3-SCR.

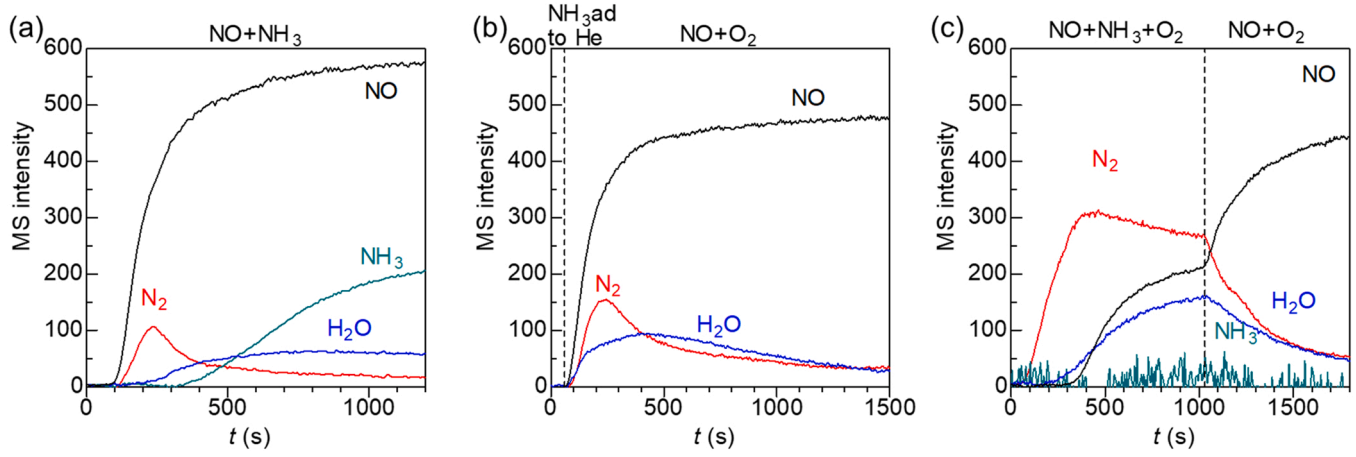

Fig. 4. Changes in the mass spectra under various gas flows ($Na_{0.33}V_2O_5$): (a) 500 ppm NO + 500 ppm NH_3, (b) NH_3 adsorption (0.1% NH_3/He) → He purge → 500 ppm NO + 8% O_2, (c) 500 ppm NO + 500 ppm NH_3 + 8% O_2 → 500 ppm NO + 8% O_2.

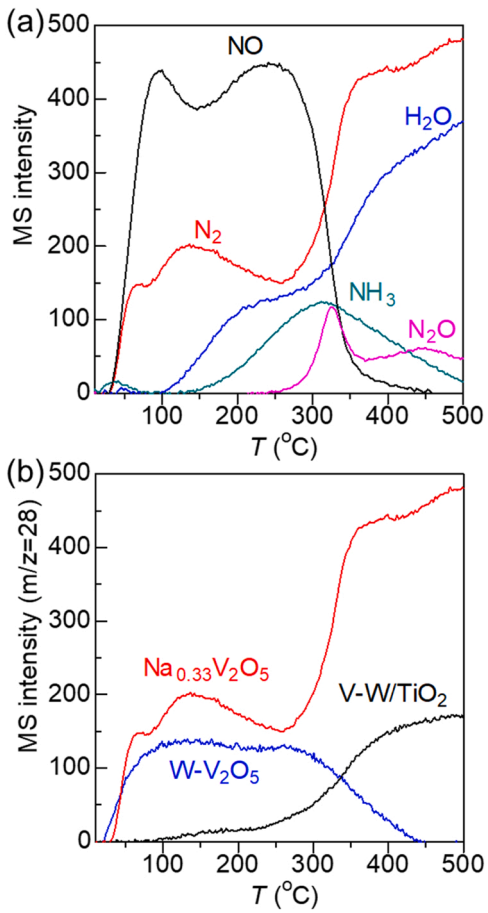

Fig. 7. (a) Temperature-programmed surface reaction (TPSR) profile of $Na_{0.33}V_2O_5$ under 500 ppm NO + 500 ppm NH_3 flow. (b) Changes in the mass spectra of N_2 ($m/z = 28$) during TPSR observation for $Na_{0.33}V_2O_5$ (16Na-V), W-V_2O_5 (W-substituted vanadium oxide) and V-W/TiO_2 (model of a conventional catalyst). Conditions: amount of the catalyst, 40 mg; programming rate, 20 °C / min.

product of NH_3-SCR. Fig. 7***b*** shows the MS intensity of N_2 ($m/z = 28$) as a function of temperature for $Na_{0.33}V_2O_5$, W-V_2O_5 (our previously reported catalyst[16]) and V-W/TiO_2 (conventional catalyst). For $Na_{0.33}V_2O_5$, two peaks (60 and 140 °C) were confirmed at a temperature lower than 300 °C. These peaks were assigned to the surface reduction of $Na_{0.33}V_2O_5$ by NH_3 + NO. The peak intensities of these peaks were larger than those of W-V_2O_5 and V-W/TiO_2 and the peak temperatures were lower than that of V-W/TiO_2. These results indicate that the reducibility of $Na_{0.33}V_2O_5$ is superior to that of W-V_2O_5 and V-W/TiO_2 under NO + NH_3 (reduction half cycle of NH_3-SCR). Na-intercalated V_2O_5 is more redox-active than are other vanadia-based catalysts and thus $Na_{0.33}V_2O_5$ showed low-temperature NH_3-SCR activity. Although the specific surface area of $Na_{0.33}V_2O_5$ (26 m^2/g) was smaller than that of W-V_2O_5 (38 m^2/g)), the MS intensity ($m/z = 28$, r.t-300°C) of $Na_{0.33}V_2O_5$ was larger than that of W-V_2O_5 as mentioned above (Fig. 7***b***). The number of active sites is large for $Na_{0.33}V_2O_5$, although the specific surface area was decreased by Na intercalation. $Na_{0.33}V_2O_5$ also showed large N_2 production peaks at a temperature of more than 250 °C. These peaks can be assigned to the bulk reduction of $Na_{0.33}V_2O_5$. These results suggest that the inner part of $Na_{0.33}V_2O_5$ is also redox active and electron transfer occurs throughout the bulk structure and is likely to be involved in the catalytic cycle because of the metallic nature of vanadium bronze.

4. Summary

In summary, we found that sodium vanadium oxide bronzes (Na-intercalated vanadium oxide) work as low-temperature NH_3-SCR catalysts. Sodium vanadium oxide bronze catalysts were synthesized by the oxalate method, and $Na_{0.33}V_2O_5$ and $Na_{1.2}V_2O_5$ were obtained as single phases. Among the synthesized catalysts, $Na_{0.33}V_2O_5$ showed 92% (dry) and 86% (wet) NO conversions at 150 °C (250 ppm NO, 250 ppm NH_3, 4% O_2, SV=40,000 mL h^{-1} g_{cat}^{-1}). The reaction rate of $Na_{0.33}V_2O_5$ (1.96×10^{-8} mol_{NO} m^{-2} s^{-1}) was 89-times higher than that of conventional V–W/TiO_2 catalyst (2.19×10^{-10} mol_{NO} m^{-2} s^{-1}). Reaction orders of $Na_{0.33}V_2O_5$ were different from those of V_2O_5 (without Na), and $Na_{0.33}V_2O_5$ (E_a=20 kJ/mol) showed a small activation energy compared to that of V_2O_5 (E_a=39 kJ/mol), suggesting different reaction mechanism. From TPD (NH_3 and NO), UV–vis and TPSR (NH_3 + NO) observations, $Na_{0.33}V_2O_5$ would proceed with NH_3-SCR by the adsorption of NH_3 and NO and redox of vanadium sites. The results indicate that alkali ions, which are normally thought to deactivate catalysts, can be promoters by changing the charge states and structure of vanadium oxide. Not only the vanadium oxides bronze catalysts but also other vanadium complex oxides might have the potential of low-temperature NH_3-SCR catalysts because of their different structural and electronic properties compared to those of V_2O_5.

CRediT authorship contribution statement

Yusuke Inomata: Data curation, Investigation, Writing – original draft, Funding acquisition. **Hiroe Kubota:** Data curation, Investigation. **Yoshinori Honmatsu:** Validation. Validation. **Hiroaki Takamitsu:** Validation. **Sosuke Sakotani:** Validation. **Kazuhiro Yoshida:Takashi Toyao:** Supervision. **Ken-ichi Shimizu:** Supervision. **Toru Murayama:** Investigation, Validation, Writing – review & editing, Funding acquisition.

Declaration of Competing Interest

The authors declare that they have no known competing financial interests or personal relationships that could have appeared to influence the work reported in this paper.

Data Availability

Data will be made available on request. The data that support the findings of this study are available from the corresponding author upon reasonable request.

Acknowledgments

This work was supported in part by the Joint Usage/Research Center for Catalysis, Hokkaido University (22AY0138 and 23AY0267), JSPS KAKENHI (20K15092) and JPNP21005, subsidized by the New Energy and Industrial Technology Development Organization (NEDO).

Appendix A. Supporting information

Supplementary data associated with this article can be found in the online version at doi:10.1016/j.apcatb.2023.122536.

References

[1] L. Han, S. Cai, M. Gao, J.Y. Hasegawa, P. Wang, J. Zhang, L. Shi, D. Zhang, Selective catalytic reduction of NOx with NH3 by using novel catalysts: state of the art and future prospects, Chem. Rev. 119 (2019) 10916–10976, https://doi.org/10.1021/acs.chemrev.9b00202.

[2] J.K. Lai, I.E. Wachs, A perspective on the selective catalytic reduction (SCR) of NO with NH3 by supported V2O5-WO3/TiO2 catalysts, ACS Catal. 8 (2018) 6537–6551, https://doi.org/10.1021/acscatal.8b01357.

[3] Y. Peng, H. Chang, Y. Dai, J. Li, Structural and surface effect of MnO2 for low temperature selective catalytic reduction of NO with NH3, Procedia Environ. Sci. 18 (2013) 384–390, https://doi.org/10.1016/j.proenv.2013.04.051.
[4] P.G. Smirniotis, D.A. Peña, B.S. Uphade, Low-temperature selective catalytic reduction (SCR) of NO with NH3 by using Mn, Cr, and Cu oxides supported on hombikat TiO2, Angew. Chem. - Int. Ed. 40 (2001) 2479–2482, https://doi.org/10.1002/1521-3773(20010702)40:13<2479::AID-ANIE2479>3.0.CO;2-7.
[5] L. Lietti, I. Nova, P. Forzatti, Selective catalytic reduction (SCR) of NO by NH3 over TiO2-supported V2O5-WO3 and V2O5-MoO3 catalysts, Top. Catal. 11–12 (2000) 111–122, https://doi.org/10.1023/A:1027217612947.
[6] P. Kornelak, D.S. Su, C. Thomas, J. Camra, A. Wesełucha-Birczyńska, M. Toba, M. Najbar, Surface species structure and activity in NO decomposition of an anatase-supported V-O-Mo catalyst, Catal. Today 137 (2008) 273–277, https://doi.org/10.1016/j.cattod.2008.03.002.
[7] S. Zhan, H. Zhang, Y. Zhang, Q. Shi, Y. Li, X.J. Li, Efficient NH3-SCR removal of NOx with highly ordered mesoporous WO3(χ)-CeO2 at low temperatures, Appl. Catal. B Environ. 203 (2017) 199–209, https://doi.org/10.1016/j.apcatb.2016.10.010.
[8] J. Zhang, Y. Liu, Y. Sun, H. Peng, X. Xu, X. Fang, W. Liu, J. Liu, X. Wang, Tetragonal rutile SnO2 solid solutions for NOx-SCR by NH3: tailoring the surface mobile oxygen and acidic sites by lattice doping, Ind. Eng. Chem. Res. 57 (2018) 10315–10326, https://doi.org/10.1021/ACS.IECR.8B02288/SUPPL_FILE/IE8B02288_SI_001.PDF.
[9] C. Liu, S. Yang, L. Ma, Y. Peng, A. Hamidreza, H. Chang, J. Li, Comparison on the performance of α-Fe2O3 and γ-Fe2O3 for selective catalytic reduction of nitrogen oxides with ammonia, Catal. Lett. 143 (2013) 697–704, https://doi.org/10.1007/s10562-013-1017-3.
[10] A. Marberger, M. Elsener, D. Ferri, O. Kröcher, VOx surface coverage optimization of V2O5/WO3-TiO2 SCR catalysts by variation of the V loading and by aging, Catalysts 5 (2015) 1704–1720, https://doi.org/10.3390/catal5041704.
[11] F. Nakajima, I. Hamada, The state-of-the-art technology of NOx control, Catal. Today 29 (1996) 109–115, https://doi.org/10.1016/0920-5861(95)00288-X.
[12] Z. Lian, J. Wei, W. Shan, Y. Yu, P.M. Radjenovic, H. Zhang, G. He, F. Liu, J.F. Li, Z. Q. Tian, H. He, Adsorption-induced active vanadium species facilitate excellent performance in low-temperature catalytic NOxabatement, J. Am. Chem. Soc. 143 (2021) 10454–10461, https://doi.org/10.1021/jacs.1c05354.
[13] Y. Inomata, S. Hata, E. Kiyonaga, K. Morita, K. Yoshida, M. Haruta, T. Murayama, Synthesis of bulk vanadium oxide with a large surface area using organic acids and its low-temperature NH3-SCR activity, Catal. Today (2020), https://doi.org/10.1016/j.cattod.2020.06.041.
[14] Y. Inomata, S. Hata, M. Mino, E. Kiyonaga, K. Morita, K. Hikino, K. Yoshida, H. Kubota, T. Toyao, K.I. Shimizu, M. Haruta, T. Murayama, Bulk vanadium oxide versus conventional V2O5/TiO2: NH3-SCR catalysts working at a low temperature below 150 °c, ACS Catal. 9 (2019) 9327–9331, https://doi.org/10.1021/acscatal.9b02695.
[15] M. Tao, S. Ishikawa, Z. Zhang, T. Murayama, Y. Inomata, A. Kamiyama, I. Nakaima, Y. Jing, S. Mine, K. Shimoda, T. Toyao, K.I. Shimizu, W. Ueda, Synthesis of zeolitic Ti, Zr-substituted vanadotungstates and investigation of their catalytic activities for low temperature NH3-SCR, ACS Catal. 11 (2021) 14016–14025, https://doi.org/10.1021/ACSCATAL.1C04086/SUPPL_FILE/CS1C04086_SI_001.PDF.
[16] M. Tao, S. Ishikawa, T. Murayama, Y. Inomata, A. Kamiyama, W. Ueda, Synthesis of zeolitic Mo-doped vanadotungstates and their catalytic activity for low-temperature NH3-SCR, Inorg. Chem. 60 (2021) 5081–5086, https://doi.org/10.1021/ACS.INORGCHEM.1C00107/SUPPL_FILE/IC1C00107_SI_001.PDF.
[17] Y. Inomata, H. Kubota, S. Hata, E. Kiyonaga, K. Morita, K. Yoshida, N. Sakaguchi, T. Toyao, K. ichi Shimizu, S. Ishikawa, W. Ueda, M. Haruta, T. Murayama, Bulk tungsten-substituted vanadium oxide for low-temperature NOx removal in the presence of water, 2021 121, Nat. Commun. 12 (2021) 1–11, https://doi.org/10.1038/s41467-020-20867-w.
[18] P.M. Marley, G.A. Horrocks, K.E. Pelcher, S. Banerjee, Transformers: the changing phases of low-dimensional vanadium oxide bronzes, Chem. Commun. 51 (2015) 5181–5198, https://doi.org/10.1039/c4cc08673b.
[19] J.K. Kim, B. Senthilkumar, S.H. Sahgong, J.H. Kim, M. Chi, Y. Kim, New chemical route for the synthesis of -Na0.33V2O5 and its fully reversible Li intercalation, ACS Appl. Mater. Interfaces 7 (2015) 7025–7032, https://doi.org/10.1021/ACSAMI.5B01260/SUPPL_FILE/AM5B01260_SI_001.PDF.
[20] A. Mukherjee, N. Sa, P.J. Phillips, A. Burrell, J. Vaughey, R.F. Klie, Direct investigation of Mg intercalation into the orthorhombic V2O5 cathode using atomic-resolution transmission electron microscopy, Chem. Mater. 29 (2017) 2218–2226, https://doi.org/10.1021/ACS.CHEMMATER.6B05089/SUPPL_FILE/CM6B05089_SI_001.PDF.
[21] N. Zhang, Y. Dong, M. Jia, X. Bian, Y. Wang, M. Qiu, J. Xu, Y. Liu, L. Jiao, F. Cheng, Rechargeable aqueous Zn-V2O5 battery with high energy density and long cycle life, ACS Energy Lett. 3 (2018) 1366–1372, https://doi.org/10.1021/ACSENERGYLETT.8B00565/SUPPL_FILE/NZ8B00565_SI_001.PDF.
[22] M. Giorgetti, M. Berrettoni, W.H. Smyrl, Doped V2O5-based cathode materials: where does the doping metal go? An X-ray absorption spectroscopy study, Chem. Mater. 19 (2007) 5991–6000, https://doi.org/10.1021/cm701910c.
[23] E.A. Esparcia, M.S. Chae, J.D. Ocon, S.T. Hong, Ammonium vanadium bronze (NH4V4O10) as a high-capacity cathode material for nonaqueous magnesium-ion batteries, Chem. Mater. 30 (2018) 3690–3696, https://doi.org/10.1021/ACS.CHEMMATER.8B00462/SUPPL_FILE/CM8B00462_SI_001.PDF.
[24] M. Schindler, F.C. Hawthorne, M.A. Alexander, R.A. Kutluoglu, P. Mandaliev, N. M. Halden, R.H. Mitchell, Na–Li–[V3O8] insertion electrodes: structures and diffusion pathways, J. Solid State Chem. 179 (2006) 2616–2628, https://doi.org/10.1016/J.JSSC.2006.05.009.
[25] Y. Lee, S.M. Oh, B. Park, B.U. Ye, N.S. Lee, J.M. Baik, S.J. Hwang, M.H. Kim, Unidirectional growth of single crystalline β-Na0.33V2O5 and α-V2O5 nanowires driven by controlling the pH of aqueous solution and their electrochemical performances for Na-ion batteries, CrystEngComm 19 (2017) 5028–5037, https://doi.org/10.1039/C7CE00781G.
[26] J. Due-Hansen, S. Boghosian, A. Kustov, P. Fristrup, G. Tsilomelekis, K. Ståhl, C. H. Christensen, R. Fehrmann, Vanadia-based SCR catalysts supported on tungstated and sulfated zirconia: influence of doping with potassium, J. Catal. 251 (2007) 459–473, https://doi.org/10.1016/J.JCAT.2007.07.016.
[27] Y. Jiang, X. Gao, Y. Zhang, W. Wu, Z. Luo, K. Cen, Effect of KCl on the selective catalytic reduction of NO with NH3 over vanadia-based catalysts for biomass combustion, Environ. Prog. Sustain. Energy 33 (2014) 390–395, https://doi.org/10.1002/EP.11795.
[28] L. Lisi, S. Cimino, Poisoning of SCR catalysts by alkali and alkaline earth metals, Page 1475, Catalysts Vol. 10 (10) (2020) 1475, https://doi.org/10.3390/CATAL10121475.
[29] X. Du, G. Yang, Y. Chen, J. Ran, L. Zhang, The different poisoning behaviors of various alkali metal containing compounds on SCR catalyst, Appl. Surf. Sci. 392 (2017) 162–168, https://doi.org/10.1016/J.APSUSC.2016.09.036.
[30] P.P. Wang, C.Y. Xu, F.X. Ma, L. Yang, L. Zhen, In situ soft-chemistry synthesis of β-Na0.33V2O5 nanorods as high-performance cathode for lithium-ion batteries, RSC Adv. 6 (2016) 105833–105839, https://doi.org/10.1039/C6RA23484D.
[31] M. Shchelkanova, G. Shekhtman, S. Pershina, E. Vovkotrub, Y. Zaikov, D. Medvedev, P. Arkhipov, O. Rakhmanova, Physico-chemical properties of NaV3O8 prepared by solid-state reaction, Page 6976, Materials Vol. 14 (14) (2021) 6976, https://doi.org/10.3390/MA14226976.
[32] H. Tang, F. Xiong, Y. Jiang, C. Pei, S. Tan, W. Yang, M. Li, Q. An, L. Mai, Alkali ions pre-intercalated layered vanadium oxide nanowires for stable magnesium ions storage, Nano Energy 58 (2019) 347–354, https://doi.org/10.1016/J.NANOEN.2019.01.053.
[33] K. Momma, F. Izumi, VESTA 3 for three-dimensional visualization of crystal, volumetric and morphology data, J. Appl. Crystallogr. 44 (2011) 1272–1276, https://doi.org/10.1107/S0021889811038970.
[34] Q. Wang, M. Brier, S. Joshi, A. Puntambekar, V. Chakrapani, Defect-induced Burstein-Moss shift in reduced V2 O5 nanostructures, Phys. Rev. B. 94 (2016), 245305, https://doi.org/10.1103/PhysRevB.94.245305.
[35] A. Marberger, D. Ferri, M. Elsener, O. Kröcher, The significance of lewis acid sites for the selective catalytic reduction of nitric oxide on vanadium-based catalysts, Angew. Chem. - Int. Ed. 55 (2016) 11989–11994, https://doi.org/10.1002/anie.201605397.